Supporting Information for

A new vanadium sulfate with interesting ferrimagnetic and NLO properties constructed from novel discrete umbrella-like $[V^{V}(\mu_3O)_4V^{IV}_4O_5(SO_4)_4(en)]^{5-}$ anions

Shuai Zhou, [a] Hongxiang Wan, [a] Gonghao Hu, [a] Ying Liu, [a] Yu Zhang, [a] Hao Miao, [a] Yan Xu *[a,b]

1. General Experimental

Data for the compounds of **1** is collected by using a Bruker Apex 2 CCD single-crystal diffractometer with Mo Kα radiation (λ = 0.710 73 Å) at 153 K using ω-2θ scan method. The single crystals of all compounds 1−3 were chosen and held on a thin glass fiber by epoxy glue in air for data collection. The SHELX software package (Bruker) was used to solve and refine the structures.[25] Absorption corrections were applied empirically using the SADABS program. All the non-hydrogen atoms were refined anisotropically. The hydrogen atoms of organic molecule were placed in calculated positions, assigned isotropic thermal parameters, and allowed to ride on their parent atoms, while the H atoms of water and disordered organic molecules were not located. All calculations were performed using the SHELX97 program package. Further details of the X-ray structural analyses for compounds **1** is given in Table. S1.

All chemicals purchased were of reagent grade and used without further purification. Powder X-ray diffraction (PXRD) were obtained on a Bruker D8X diffractometer equipped with monochromatized Cu Kα (λ = 1.5418 Å) radiation at room temperature. Data were collected in the range of 5−50°, and the experimental XRD patterns are in agreement with the patterns simulated on the basis of the single-crystal structures. The infrared (IR) spectra were recorded on a Nicolet Impact 410 FTIR spectrometer using KBr pellets in the 4000-500 cm^{-1} region. C, H, and N elemental analyses were performed on a PerkinElmer 2400 CHN elemental analyzer. Quantum Design MPMS SQUID magnetometer using single-crystal samples at temperatures ranging from 2 to 300 K. The direct current measurements were collected using applied fields in the range of 0-7 T. The alternating current (AC) measurements were used to analyze a possible frequency dependence of the real and imaginary part of the magnetic susceptibility with amplitudes of 2 Oe in the frequency range from 1.2 to 300 Hz. Data were corrected for contributions for the sample holder and for the diamagnetism according to the Pascal constants.

2. Syntheses of complexe 1.

A mixture of $VOSO_4 \cdot xH_2O$ (0.1185 g, x = 3 or 4), 1,2-ethylenediamine (en) (0.0119 g, 0.198 mmol),and H_2SO_4 (98 wt%, 0.2891 g, 2.891 mmol) were added into 7ml N,N-Dimethylformamide (DMF) and stirred for two hours, then the mixture was sealed into a 25 ml Teflon-lined autoclave and heated to 180 °C for 5 days. After

cooling to room temperature, the product was filtered off, and washed with alcohol, then dark green block crystals was obtained (Yield: 0.0416g, 33.25% based on V). Elemental analysis found (%): C, 16.43; H, 5.37; N, 10.63 (Calcd. (%): C, 16.70; H, 5.54; N, 10.86). IR of compound 1 (cm^{-1}): 3441 (vs), 2780 (m), 1626 (m), 1387 (w), 1326 (s), 1185 (m), 1022 (w), 987 (m), 765 (w), 708 (w).

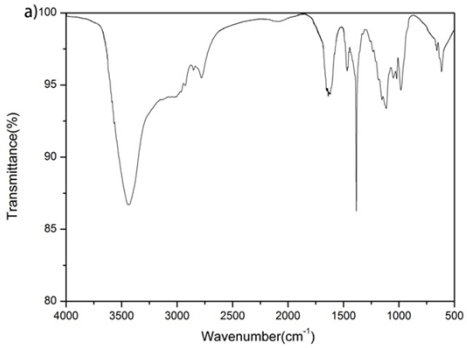

Fig. S1 The IR spectra of complex **1**

Infrared (IR) spectra were recorded on a Nicolet Impact 410 FTIR spectrometer using KBr pellets in the 4000-500 cm^{-1} region. The spectrum for **1** was shown in Fig. S2. For compound **1**, the band at 987 cm^{-1} as well as 708 cm^{-1} can be assigned to ν(V=O) or ν(V-O-V) and ν(V-O) vibrations while the peaks from 1326 cm^{-1} to 1626 cm^{-1} may be ascribed to the characteristic absorption band for ethylenediamine. The bands associated with the ν(N-H) and ν(C-H) appeared at 2780 and 3441 cm^{-1}.

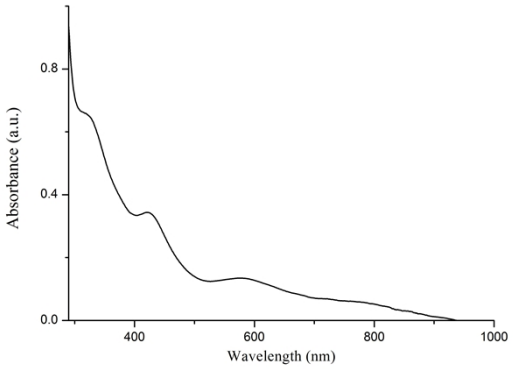

Fig. S2 UV-VIS spectra of the compound **1**

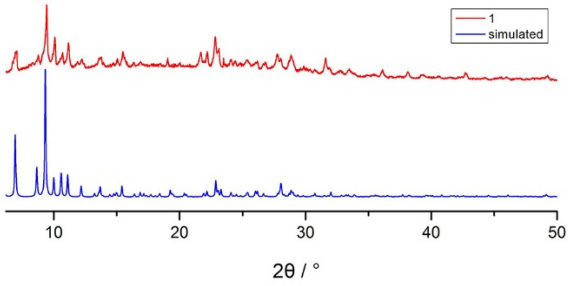

Fig. S3 The experimental and simulated XRD patterns for 1

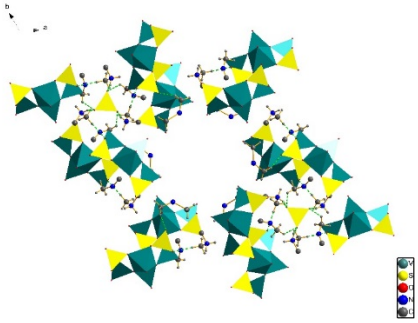

Fig. S4 Structure of **1** along the [001] direction showing the interaction between the amine and the inorganic core

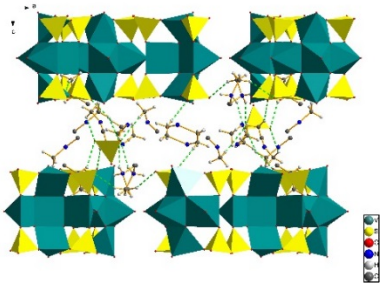

Fig. S5 Structure of **1** along the *c*-axis showing the interaction between the amine and the inorganic core leading to a layer-like network. Green dotted line: hydrogen bonds

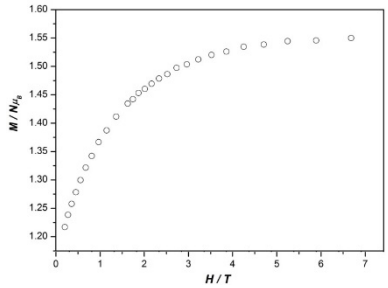

Fig. S6 Field dependence of magnetization for 1 meansured at 1.8 K.

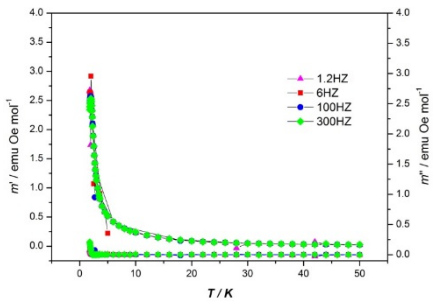

Fig. S7 Temperature variation of the in-phase m' and out-of-phase m'' produucts for 1 at frequencies 1.2-300 Hz under a 2 Oe AC filed

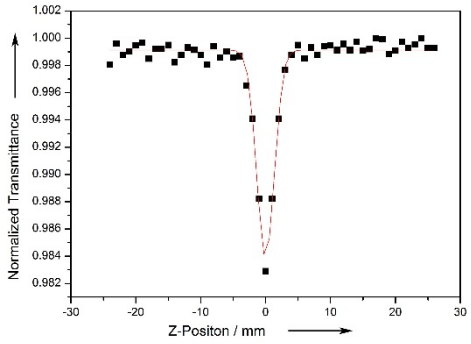

Fig. S8 The open aperture z-scan data at 720 nm for compound **1** in water at 3.5×10^{-4} mol L^{-1}. The unfilled circles are the experimental data and the solid curve represents the theoretical data.

The electronic spectrums of compounds **1** in water at a concentration of 3.5×10^{-4} mol·L^{-1} give the liner absorption at room temperature. Two-photon absorption (TPA) values containing TPA coefficient β and TPA cross section σ were measured by the open-aperture *Z*-scan technique with femtosecond laser pulse and Ti:95 sapphire system (720 nm, 80 Hz, 140 fs). Figures S7 shows the open aperture Z-scan curves of compounds **1** The unfilled circles are the experimental data and the solid line represents the theoretical simulated curve modified by the following equations:

$$T(z,s=1)=\sum_{m=0}^{\infty}\frac{[-q_0(z)]^m}{(m+1)^{3/2}} \quad \text{for} \quad |q_0|<1 \qquad (1)$$

$$q_0(z)=\frac{\beta I_0 L_{eff}}{1+z^2/{z_0}^2} \qquad (2)$$

where β is the TPA cofficient of the solution, I_0 is the input intensity of laser beam at the focus $z = 0$, $L_{eff} = (1\text{-}e^{-\alpha L})/\alpha$ is the effective length with α and L are the linear absorption coefficient and the sample length respectively. z is the sample position, $z_0 = \pi\omega_0^2/\lambda$ is the diffraction length of the beam, in which the ω_0 and λ are the spot size at the focus and the wavelength of the beam respectively. By using the equations mentioned above, we deduce the TPA absorption coefficient β are calculated as 0.005278 cm/GW for compounds **1** Furthermore, the molecular TPA cross section σ can be calculated by the following relationship:

$$\sigma N_A d\times10^{-3}=h\nu\beta \qquad (3)$$

where N_A, d, h and v are respectively the Avogadro's constant, the concentration of the compound, the Planck's constant and the frequency of input intensity. Based on Eq. (3), the molecular TPA cross section σ of compounds **1** were calculated as 622 GM (1 GM = 10^{-50} cm^4s/photon).

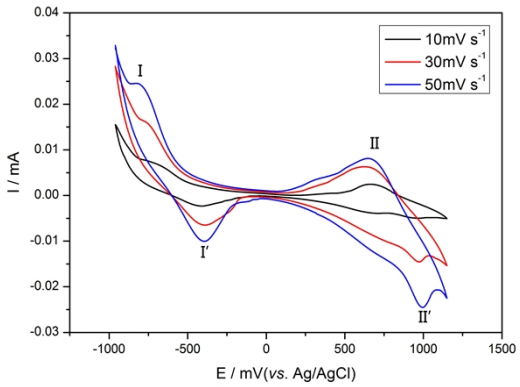

Fig. S9 CV curves of **1** with the concentration of 3×10^{-4} M in a pH = 0.2 M KCl solution were detected in every 2 hours and totally detected for three times at the scan rate of 10 mV s^{-1}, 30 mV s^{-1} and 50 mV s^{-1}. A bulk-modified carbon paste electrode as a working electrode, a platinum-wire auxiliary electrode, and an Ag/Ag^{+} wire reference electrode.

A cyclic voltammogram of **1** has been shown in Fig S9. For compound **1**, at a scan rate of 30 mVs^{-1}, in the forward potential sweep, two processes are visible at -410 mV (E_{pa}) and 960 mV (E_{pa}) vs Ag/Ag^{+} while two processes are represented at -780 mV (E_{pc}) and 656 mV (E_{pc}) on the reverse sweep. POVs exhibit CV reduction waves correspond to the high oxidation state of the vanadium (a mixed valence combination of d^0 and d^1). Electrochemical reduction is accompanied by electron transfer from non-bridging (terminal) oxygen surface atoms to the d^0 and d^1 polyhedral vanadium atoms through the $V{=}O_t$ dπ–pπ interaction. The splitting between the procedure indicates that the vanadium centers interact electronically and all processes are electronically equivalent and quasi-reversible. The presence of two processes support the existence of two crystallographically distinct vanadium atoms (with valencies of 4+ and 5+ from BVS calculations). In addition, the mean peak potentials $E_{1/2} = (E_{pa}+E_{pc}) / 2$ is 758 mV, which can be assigned to V^{IV}/V^{V}, whereas the other mean peak potentials is -595 mV, which can be ascribed to V^{III}/V^{IV}. We also measure the CV (cyclic voltammetric) behaviors of compound **1** at the other scan rates (10 and 50 mV s^{-1}). And we observed that no obvious voltammetric characteristics have ever changed in the CV curves. The results can confirm that compound **1** is structurally stable in the aqueous solution. In summary, both two compounds showed the excellent electrochemical property of V^{IV}/V^{V} and V^{III}/V^{IV}

couples.

Table. S1. Crystal data and structure refinements for **1**

Compound	1
formula	$C_{16}H_{63.33}N_9O_{27.67}S_{4.67}V_5$
fw	1229.07
T (K)	296(2)
Wavelength (Å)	0.71073
cryst syst	hexagonal
space group	$P6_3/m$
a (Å)	20.4115(17)
b (Å)	20.4115(17)
α (deg)	90
β (deg)	90
γ (deg)	120
V Å^3	9180.3(17)
Z	6
Dc (Mg m^{-3})	1.347
μ (mm^{-1})	0.969
F(000)	3839
Crystal size (mm)	0.15 x 0.13 x 0.12
θ range (deg)	1.60-25.02
Limiting indices	-23≤h≤21 -9≤k≤24 -12≤l≤30
reflns collected	16084
indep reflns	5460
Data/restraints/params	5460 / 192 / 392
GOF	1.052
R1[a], wR2[b] [I>2σ(I)]	0.0703, 0.1862
R1, wR2 (all data)	0.1121, 0.2131

[a] $R1 = \Sigma||F_o| - |F_c||/\Sigma|F_o|$. [b] $wR2 = \Sigma[w(F_o^2 - F_c^2)^2]/\Sigma[w(F_o^2)^2]^{1/2}$.

Table. S2. Selected bond lengths [A] and angles [deg] for **1**[a]

V(1)-O(8)	1.581(5)	V(4)-O(14)	1.972(5)
V(1)-O(3)	1.978(3)	V(4)-O(14)#1	1.972(5)
V(1)-O(3)#1	1.978(3)	V(4)-O(4)#1	1.973(4)
V(1)-O(9)	1.990(4)	V(4)-O(4)	1.973(4)
V(1)-O(9)#1	1.990(4)	S(1)-O(12)	1.445(4)
V(2)-O(13)	1.590(6)	S(1)-O(11)	1.455(4)
V(2)-O(3)#1	1.855(4)	S(1)-O(10)	1.496(4)
V(2)-O(3)	1.855(4)	S(1)-O(9)	1.513(4)
V(2)-O(4)	1.887(4)	S(2)-O(17)	1.463(8)
V(2)-O(4)#1	1.887(4)	S(2)-O(18)	1.475(6)
V(3)-O(6)	1.584(4)	S(2)-O(18)#2	1.475(6)
V(3)-O(4)	1.943(4)	S(2)-O(18)#3	1.475(6)
V(3)-O(3)	1.963(3)	S(3)-O(1)	1.444(6)
V(3)-O(16)	1.978(4)	S(3)-O(2)	1.471(6)
V(3)-O(10)	2.007(4)	S(3)-O(14)	1.506(5)
V(4)-O(5)	1.610(6)	S(3)-O(16)	1.526(4)
O(8)-V(1)-O(3)	105.69(18)	O(16)-V(3)-O(10)	83.29(17)
O(8)-V(1)-O(3)#1	105.69(18)	O(5)-V(4)-O(14)	104.8(2)
O(3)-V(1)-O(3)#1	78.2(2)	O(5)-V(4)-O(14)#1	104.8(2)
O(8)-V(1)-O(9)	103.61(18)	O(14)-V(4)-O(14)#1	85.9(3)
O(3)-V(1)-O(9)	90.15(15)	O(5)-V(4)-O(4)#1	104.8(2)
O(3)#1-V(1)-O(9)	150.42(16)	O(14)-V(4)-O(4)#1	150.14(18)
O(8)-V(1)-O(9)#1	103.61(18)	O(14)#1-V(4)-O(4)#1	89.95(16)
O(3)-V(1)-O(9)#1	150.42(16)	O(5)-V(4)-O(4)	104.8(2)
O(3)#1-V(1)-O(9)#1	90.15(15)	O(14)-V(4)-O(4)	89.95(16)
O(9)-V(1)-O(9)#1	86.9(2)	O(14)#1-V(4)-O(4)	150.14(18)
O(13)-V(2)-O(3)#1	109.16(19)	O(4)#1-V(4)-O(4)	79.1(2)
O(13)-V(2)-O(3)	109.16(19)	O(12)-S(1)-O(11)	114.2(3)
O(3)#1-V(2)-O(3)	84.5(2)	O(12)-S(1)-O(10)	108.0(2)
O(13)-V(2)-O(4)	109.1(2)	O(11)-S(1)-O(10)	110.1(2)
O(3)#1-V(2)-O(4)	141.73(17)	O(12)-S(1)-O(9)	107.8(2)
O(3)-V(2)-O(4)	83.63(16)	O(11)-S(1)-O(9)	110.2(2)
O(13)-V(2)-O(4)#1	109.1(2)	O(10)-S(1)-O(9)	106.1(2)
O(3)#1-V(2)-O(4)#1	83.63(16)	O(17)-S(2)-O(18)	108.5(3)
O(3)-V(2)-O(4)#1	141.73(17)	O(17)-S(2)-O(18)#2	108.5(3)
O(4)-V(2)-O(4)#1	83.6(2)	O(18)-S(2)-O(18)#2	110.4(3)
O(6)-V(3)-O(4)	106.7(2)	O(17)-S(2)-O(18)#3	108.5(3)
O(6)-V(3)-O(3)	105.3(2)	O(18)-S(2)-O(18)#3	110.4(3)
O(4)-V(3)-O(3)	79.37(15)	O(18)#2-S(2)-O(18)#3	110.4(3)
O(6)-V(3)-O(16)	105.0(2)	O(1)-S(3)-O(2)	113.7(4)
O(4)-V(3)-O(16)	90.28(16)	O(1)-S(3)-O(14)	109.6(3)
O(3)-V(3)-O(16)	149.62(17)	O(2)-S(3)-O(14)	110.0(3)

O(6)-V(3)-O(10)	105.8(2)	O(1)-S(3)-O(16)	107.1(3)
O(4)-V(3)-O(10)	147.43(16)	O(2)-S(3)-O(16)	109.6(3)
O(3)-V(3)-O(10)	90.23(15)	O(14)-S(3)-O(16)	106.6(2)

[a] Symmetry transformations used to generate equivalent atoms: （#1） x, y, -z+1/2；(#2) -y+1, x-y, z; (#3) -x+y+1, -x+1, z.

Table. S3. Hydrogen Bonds (Angstrom, Deg) for **1**

D-H...A	*d*(D...A)	∠(DHA)
N1–H1A...O17	2.928(6)	152.00
N1–H1A...O18	3.079(9)	142.00
N1–H1B...O3	3.250(7)	137.00
N1–H1B...O11	2.906(8)	136.00
N2A–H...O3	2.92(2)	
N2A–H...O4	2.96(2)	
C2–H2A...O8	3.166(10)	133.00
C1C–H1CB...O18	3.23(2)	133.00
C4–H4C...O2	3.37(4)	148.00
C5–H5B...O6	3.294(19)	165.00
C5–H5C...O12	3.36(2)	156.00

.